Carbohydrate Polymers 111 (2014) 524–529

Contents lists available at ScienceDirect

Carbohydrate Polymers

journal homepage: www.elsevier.com/locate/carbpol

Reactive coating of soybean oil-based polymer on nanofibrillated cellulose film for water vapor barrier packaging

Peng Lu [a], Huining Xiao [a,*], Weiwei Zhang [a,b], Glen Gong [a,c]

[a] Department of Chemical Engineering and Limerick Pulp & Paper Centre, University of New Brunswick, Fredericton NB E3B 5A3, Canada
[b] State Key Laboratory of Pulp and Paper Engineering, South China University of Technology, Guangzhou 500640, PR China
[c] Department of Chemical Engineering, University of Waterloo, Waterloo, Ontario N2L 3G1, Canada

ARTICLE INFO

Article history:
Received 29 December 2013
Received in revised form 8 April 2014
Accepted 13 April 2014
Available online 27 April 2014

Keywords:
Nanofibrillated cellulose
Acrylated epoxidized soybean oil
Water vapor transmission rate

ABSTRACT

Nanofibrillated cellulose (NFC) easily forms a high strength film but is unable to withstand the influence of water vapor when used in high moisture situations. The water vapor transmission rate (WVTR) of a NFC film was as high as 5088 g/m^2 24 h (38 °C, 90% RH). The addition of beeswax latex in a NFC casting film (NFX) lowered the WVTR to 3918 g/m^2 24 h. To further reduce the WVTR, a coating agent comprised of acrylated epoxidized soybean oil (AESO) and 3-aminopropyltriethoxysilane (APTS) was applied onto the NFX film using a rod coater. A combination of the suitable AESO/APTS ratio, initiator dosing, curing time and temperature could reduce the WVTR to 188 g/m^2 24 h when the coat weight was 5 g/m^2. Moreover, the coated NFX film was highly hydrophobic along with the improved transparency and thermal stability. This biodegradable polymer-coated NFC film can be used as potential packaging barrier in certain areas.

1. Introduction

Packaging plays an important role in production, transportation and storage of food or pharmaceutical. This requires the packaging material to have a low water vapor transmission rate (WVTR). The most commonly-used packaging material nowadays is petrochemical-based plastics such as polyolefins, polyesters, and polyamides, which do own low WVTR feature but they are totally non-biodegradable. As thousands of tons of these plastic packagings are discarded daily and most of them are normally put in land-fills, they increasingly lead to serious ecological problems.

Nanofibrillated cellulose (NFC) is a renewable material from nature resources. The key advantages in use of NFC are its super strength and numerous free reactive hydroxyl groups on its surface that can be functionalized. In addition, NFC shows a good film-forming capacity which qualifies it for applications in packaging fields in the form of large scale films (Tammelin, Hippi, & Salminen, 2013), nanopaper (Sehaqui, Liu, Zhou, & Berglund, 2010), or nanocomposite (Larsson, Berglund, Ankerfors, & Lindström, 2012). However, a huge amount of hydroxyl groups on the NFC surface result in poor water vapor barrier properties in NFC films (Spence, Venditti, Rojas, & Hubbe, 2011). The common approaches to improve the moisture barrier capacity of NFC films for packaging applications are to treat the surfaces of NFC substrates with a synthetic polymer such as petrochemical-based plastics, or biopolymer (e.g. whey proteins, polycaprolactone, poly (lactic acid), beeswax) (Lavoine, Desloges, Dufresne, & Bras, 2012; Zhang, Xiao, & Qian, 2014), or inorganic impermeable particles like mica (Alves, Costa, & Coelhoso, 2010) or montmorrilonite (Liu & Berglund, 2012) through laminating extrusion, vacuum deposition, and multilayer coating (Andersson, 2008; Ham-Pichavant, Sebe, Pardon, & Coma, 2005). In consideration of the packaging waste disposal problems, it is preferred to choose a material which has a high moisture barrier capacity and a potential biodegradability when compared to the products from petroleum. Acrylated epoxidized soybean oil (AESO), a soybean oil derivate monomer, is an interesting polymeric material obtained from renewable natural resources, which has acrylate functional groups to polymerize/copolymerize easily via a free-radical reaction under several initiator systems. However, a pure AESO polymer (poly-AESO) behaves like an amorphous cross-linked rubber, which fails to by itself produce suitable shapes giving high mechanical properties (López & Santiago, 2013). Studies reveal that under the controlled polymerization or co-polymerization with other chemical species (such as vinyl monomers, organofunctional alkoxysilanes, diamines, anhydrides, and isocyanates), the resulting polymers could have optimized properties, which could be widely used as surface coating and adhesive agents (Çolak & Küsefoğlu, 2007; Grishchuk & Karger-Kocsis, 2011). These

* Corresponding author. Tel.: +1 5064533532; fax: +1 5064533591.
E-mail address: hxiao@unb.ca (H. Xiao).

http://dx.doi.org/10.1016/j.carbpol.2014.04.071
0144-8617/

Table 1
Effect of the APTS content on the film qualities in terms of soluble fraction, WVTR (38 °C, 90% RH), wettability (contact angle) and surface roughness.

Sample[a] #	APTS (%)[b]	Soluble fraction (%)	WVTR[c] (g/m² 24 h)	Contact angle (°)	Roughness (nm)[d]
NFC	–	–	5088 ± 3	67.0 ± 0.3	17
NFX	–	–	3918 ± 2	93.7 ± 0.5	29.7
A1	10	50.7 ± 0.25	2513 ± 2	95.7 ± 0.7	1.39
A2	20	29.1 ± 0.53	2301 ± 7	102.6 ± 0.2	0.65
A3	30	21.5 ± 0.41	1714 ± 7	103.9 ± 0.3	7.44
A4	40	24.6 ± 0.17	1826 ± 3	94.2 ± 0.7	5.61
A5	50	23.8 ± 0.14	1910 ± 2	92.3 ± 0.4	1.72

[a] The BPO content in the coating fluid, the curing temperature and the curing time were fixed to 1 wt%, 80 °C and 30 min, respectively.
[b] APTS/AESO weight percentage.
[c] The coat weight was fixed to 1.0 g/m².
[d] Mean roughness (R_a) was measured within the 1 μm × 1 μm AFM image.

AESO-based polymers are also expected to have a good moisture barrier capacity due to their good film-forming and hydrophobic properties. However, AESO in cellulose film or fiber network in packaging manufacture has seldom been used to date.

The objective of this work was to fabricate a NFC-based packaging material of a highly effective water vapor barrier capacity. Thin films cast from NFC suspension with beeswax latex as a hydrophobic additive were used as substrate (NFX). To enhance the water vapor barrier capacity of film substrates, a reactive coating agent consisting of AESO was applied on top of the NFX film. After curing in suitable condition, a hydrophobic water vapor barrier layer was expected to form on the top of the NFX film.

2. Materials and methods

2.1. Materials

Nanofibrillated cellulose (NFC) with an average width around 20 nm and several micrometers in length was obtained from the University of Toronto (aqueous suspension of solid content at 0.6 wt%). Beeswax latex was used as a hydrophobic additive in NFC casting films and prepared in our lab with chitosan as a dispersing agent. In the coating formulation, acrylated epoxidized soybean oil (AESO) was used as a monomer which contains 3 to 4 acrylate double bonds per molecule on average; benzoyl peroxide (BPO) was used as an initiator to induce the free radical polymerization of AESO. A mixture of acetone and ethanol was used as a diluent. 3-aminopropyltriethoxysilane (APTS) and other reagents were commercially available and used as received.

2.2. Preparation of films and surface reactive coating

The NFC film was prepared by pouring the NFC suspensions into polystyrene petri dishes then allowing them to dry at a temperature of 23 °C and a relative humidity (RH) of 50%. Following the same procedure, NFX film was prepared with the beeswax latex as an additive in the NFC suspension before casting and the solid beeswax content in the NFC suspension was 10.0 wt% (on the dry NFC). In this study, the grammage (g/m²) of the NFC film and NFX film were both fixed at 10 g/m².

The NFX film was chosen as the base film for coatings due to its better hydrophobicity compared with the NFC film (Table 1). A coating fluid which consists of varied AESO, BPO and APTS was applied onto the NFX film using a rod coater (K303 Multicoater, RK. Print Coat Instruments Ltd., UK) at a velocity of 3 m/min. Immediately after the coating, the films were put into the oven for curing for different durations at a specific temperature. The same procedure was repeated at different temperatures (Fig. 3). Triple repeats were performed for each temperature and time. The coat weight was controlled at 1 g/m², 3 g/m² and 5 g/m² using different rods for coating. The reaction of the coating fluid on the NFX surface was characterized with attenuated total reflectance-fourier transform infrared (ATR-FTIR) using a NEXUS 470 spectrophotometer (Nicolet Thermo Instruments Inc., Canada). The spectra were recorded in the absorption band mode in the 4000 cm^{-1} to 450 cm^{-1} range.

2.3. WVTR measurement

The water vapor transmission rate (WVTR) is defined as the steady water vapor flow in unit time through unit area of a body to specific parallel surfaces under specific conditions of temperatures and humidity. WVTR was evaluated by the modified water method according to the standard ASTM E96 (2000) and ASTM D1653-03 (2003). In this study, the specimen was attached to the test dish containing saturated potassium nitrate (KNO_3) solution which keeps the relative humidity (RH %) inside of the assembled test dishes at 90%. The chamber where the assembled test dishes were to be placed had a temperature maintained constant at 38 °C and relative humidity at 0% controlled by anhydrous calcium chloride (Desiccant) in the form of small lumps. The dish assembly was weighed periodically and the changes in the weight were plotted as a function of time. The slope was calculated by linear regression method and the WVTR (g/m² 24 h) was calculated from the slope of the straight line (g/h) divided by the transfer area (m²) (Cerpakovska & Kalnins, 2012; Prakash Marana, Sivakumar, Sridhar, & Thirugnanasambandham, 2013).

2.4. Characteristics of the films

The soluble fraction of the coating was determined by immersing the cured sample (W_0) in acetone at 25 °C. After 24 h., the sample was filtered out and dried in a vacuum oven at 50 °C until constant weight (W_1) was achieved. The soluble fraction was calculated by the following equation: soluble fraction (%) = $[1 - (W_1/W_0)] \times 100\%$. Generally, the higher the conversion of the monomers to polymer, the lower soluble fraction removed after acetone extraction; and correspondingly the better the barrier layer was obtained. The tensile strengths (N/m) of the films were measured according to TAPPI T494 om-01 (2006) and the tensile index (N m/g) was obtained by dividing the tensile strength with the film grammage. The static contact angles of water droplets (3 μl) on the films were measured using an Attension Theta Optical Tensiometer (Finland). Ten measurements were made on each sample. To determine the morphology of the samples, atomic force microscopy (AFM) measurements were performed using a Nanoscope IIIa from Veeco Instruments Inc., Santa Barbara, CA. The images were scanned in Multimode mode in air using a commercial silicon tapping probe (NP-S20, Veeco Instruments) with a resonance frequency of about 273 kHz. The roughness measurement was taken from the AFM image by the arithmetic average of absolute values of the surface height deviations measured from the mean plane within the box

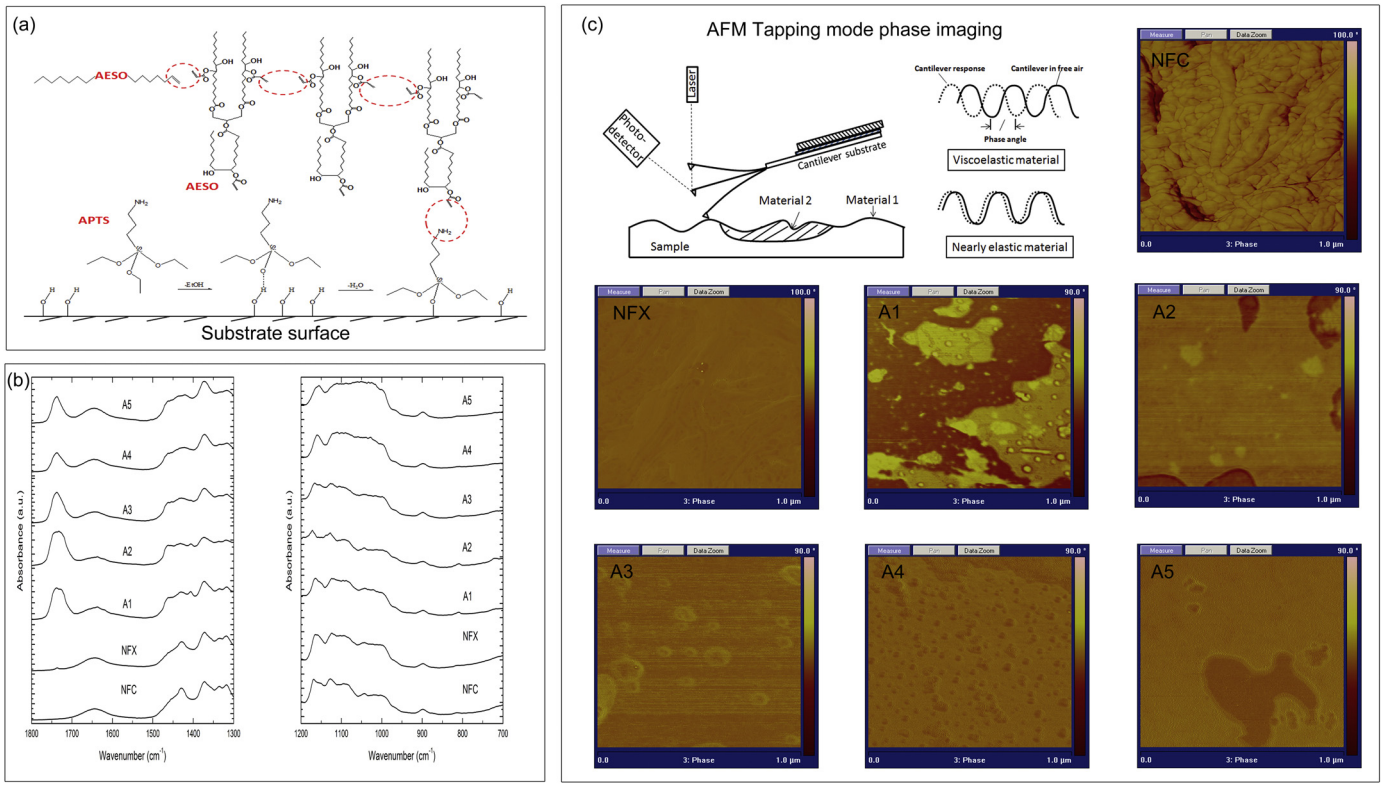

Fig. 1. (a) Scheme of the chemical reaction of the coating on the NFX film when curing; (b) (ATR) FT-IR spectra of the coated NFX film at different APTS content; (c) AFM tapping mode phase images of the coated NFX film at different APTS content.

cursor. The cross section of the films was examined with scanning electron microscopy (JEOL 6400 SEM, JEOL Ltd., Japan). An accelerating voltage of 15 kV was used to scan the samples.

2.5. Thermal stability and optical property

Thermal properties of films were determined using a TA Instruments Calorimeter Q200 (TA Instruments Ltd., Leatherhead, UK) with a nitrogen differential scanning calorimetry (DSC) cell purge at 100 ml/min. Samples were conditioned at 50% RH and 23 °C for 48 h and were then heated from 20 to 700 °C at 20 °C/min. The regular light transmittances of the films were measured at wavelengths from 200 to 700 nm using an ultraviolet (UV)-visible spectrometer (Genesys 10-s, Thermo Electron Corporation, USA).

3. Results and discussion

WVTR is the standard measurement by which films are compared for their ability to resist moisture transmission at specified conditions of temperature and relative humidity. Lower WVTR values indicate better moisture barrier property. The barrier performance of the coated NFX films was determined mainly by the quality of the coating layer. The curing of the coating fluid after applying on the NFX film was believed to involve two reactions, Fig. 1(a). On the one hand, AESO, the main constituent in the coating fluid, could go through chain propagation to form a polymer due to its sufficient acrylate groups. On the other hand, the residual double bonds on the AESO skeleton can be reactive to APTS through a Michael addition reaction (Çolak & Küsefoğlu, 2007). Finally, the coating layer after curing would have a large triglyceride skeleton rendering the interface hydrophobic and a reactive silanol group for covalent bonding with the hydroxyl groups on the surface of NFX film through condensation on the other hand (Marquez, Grady, & Robb, 2005). Based on this assumption, the coating formulation such as monomer ratio, initiator ratio, reaction temperature and time will determine the quality of the barrier layer during the curing process.

3.1. Effect of APTS content on the coating property

Considering the fact that AESO yields rubber-like materials when cured alone, APTS was introduced in the coating formulation as a reactive comonomer. APTS is a bifunctional compound that possesses both the amino end which is capable of reacting with AESO and the ethoxy silane end which can be hydrolyzed to silanols and then reacted with hydroxyl bearing surfaces. The detailed information about how the film qualities were affected by the APTS content is shown in Table 1.

Table 1 shows that the WVTR of the NFC film was fairly high (5088 g/m^2 24 h) with a contact angle as low as 67° because of the hydrophilic nature of the NFC fibers. The NFX film which contained beeswax as a hydrophobic additive had an improved water vapor barrier property only to some extent (3918 g/m^2 24 h) even though the contact angle increased to 93°. On the contrary, after surface reactive coating, the WVTR was reduced significantly. It was clearly seen that as the APTS content increased, the WVTR of the coated NFX first decreased to the lowest value (1714 g/m^2 24 h) and then went up.

When the APTS content was rather low (10 wt% of the AESO), the reduction in the WVTR was not very obvious compared with the uncoated NFX film. This is because most of the monomers were not participating in the reaction during the curing, which could be confirmed from a high soluble fraction of the film (50.7%) and a low contact angle (95.7°). Continued increase in the APTS content led to a reduction in the WVTR value and an increase in the film hydrophobicity (high contact angle). The best result appeared at ATPS 30 wt% and the resulting WVTR was as low as 1714 g/m^2 24 h. Further increase in the ATPS content will not give remarkable reduction

in the WVTR due to the formation of incompact network by the reaction between AESO and APTS. Moreover, the formed barrier layer, sample A3, showed a fairly good hydrophobicity, which was confirmed by its higher contact angle than the others.

The role of the APTS in the coating formulation during curing could also be revealed by the ATR-FTIR spectra and the AFM phase image of the coated NFX film. In the ATR-FTIR spectrum of coated NFX film, Fig. 1(b), when the APTS content increased (from A1 to A5), there was a disappearance trend of stretching vibrations of C=C double bonds at 1623 cm^{-1} and the bending vibration of =C—H (the double bonds on AESO) at 810 cm^{-1}, implying that the chain propagation of the AESO and the Michael addition reaction between AESO and APTS took place. As the APTS content increased, the absorption bands at 3300 cm^{-1} of the primary amines first decreased in intensity and then increased. This is because APTS could covalently couple with AESO at a low content, but when the APTS content is higher than 30 wt%, the primary amines on the excessive APTS cannot go through Michael addition with AESO. The successful covalent coupling of AESO to APTS was also proved by the presence of the peaks between 1550 and 1650 cm^{-1}, corresponding to the >N-H group of the silanized-AESO (Coates, 2013). Subsequent to the polymerization and Michael addition, the siloxane condensation could be indicated by the changes of the asymmetric and symmetric deformation modes of the CH_3 group from ethoxy moieties of APTS observed around 1440 and 1390 cm^{-1}, respectively (Kim, Seidler, Fill, & Wan, 2008). The characteristic absorption peaks at 1123 cm^{-1} and 1020 cm^{-1} are related to Si—O—Si and Si—O—C stretching and further support the chemical reaction between silane and the NFX film.

An AFM phase image is a record of the phase lagging of the cantilever oscillation versus the phase of the driving signal. It is an indication of the energy loss during the 'tapping' motion of the tip on top of the sample. Different degrees of phase lagging indicate a sample surface with different degrees of softness or vertical adhesion (Park, Xu, & Seetharaman, 2011). Phase angle images give information that cannot be obtained from topography or friction images (Scott & Bhushan, 2003). For instance, the phase image of the NFX shown in Fig. 1(c) seems much smoother without any visible phase angle contrast compared with the NFC, even though the roughness of the NFX (R_a = 29.7 nm) is higher than that of the NFC (R_a = 17). Fig. 1(c) shows AFM phase contrast for the coated NFX film of different APTS contents. The phase separation was observed beginning at APTS content 10 wt% and manifested itself in unreacted AESO or poly-AESO as bright domains (viscoelastic) of larger phase shift (in phase mode) surrounded by a matrix (cross-linked AESO-APTS) of lower phase shift. The change in the phase contrast is directly corresponding to the WVTR values. As the bright domain in A1 was assigned to the unreacted AESO or poly-AESO, it is notorious in water vapor barrier and therefore is recognized as a defect in the coated film. As the APTS content increased (from A1 to A3), more AESO were involved in the reaction with APTS, which finally reduced the bright domains in the matrix and correspondingly resulted in a decrease in WVTR. However, after APTS content was over 30 wt%, the domain shape and composition changed and at last a large number of smaller islands (self-assembled APTS) were clearly visible among the matrix for APTS content of 40 wt% (A4). As the APTS content continued increased to 50 wt% (A5), APTS patches appeared as a second phase existing amidst the continuous phase. Finally, the water vapor barrier property of the coated NFX film was flawed by those unreacted APTS patches. (Sanchez & Badia, 2003).

3.2. Effect of BPO content on the coating property

Apart from the effect of APTS content on the coating property, the BPO content (wt% of the total monomers) also plays an important role in the water vapor barrier property of the coated NFX film. Fig. 2 shows how the WVTR, soluble fraction, and CA of the coated NFX film varied at different BPO contents. All the experiments were conducted at a fixed APTS content (30 wt%), reaction temperature (80 °C) and time (30 min) with the coat weight fixed at 1 g/m^2. When the content of the initiator BPO in the coating formulation increased, the WVTR of the coated NFX film first decreased to the lowest value (1517 g/m^2·24 h) and then went up. This result can be explained by the change of the soluble fraction with the BPO content which followed a similar trend as the WVTR. When the BPO content was lower than 0.4 wt%, around 23% of the monomers were unreacted (soluble fraction) and the contact angle of the coated film was rather low (97.4°). After increasing the BPO content to 0.4 wt%, less soluble fraction was detected from the coated film and, therefore, formed coating was more compacted which had a better water vapor barrier property and a higher contact angle (105.1°). Further increase in the BPO content will not continually reduce the soluble fraction in the coated NFX film and, therefore, both the WVTR result and the contact angle did not changed so much. In conclusion, the best content of the BPO in the coating formulation is 0.4 wt%.

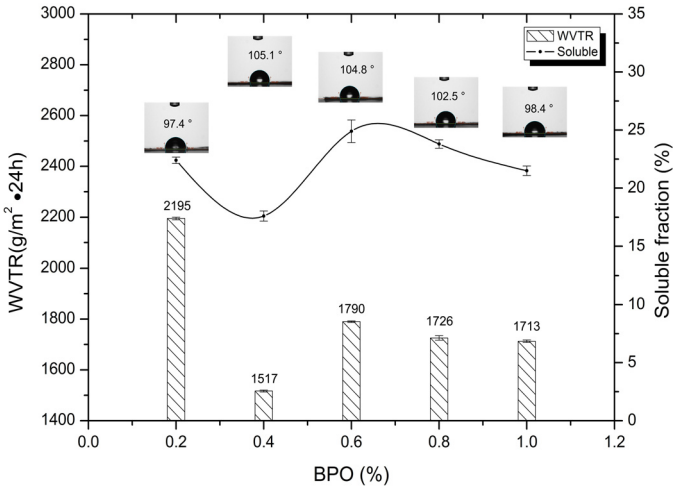

Fig. 2. WVTR, soluble fraction and CA of the coated NFX film at different BPO contents.

3.3. Effect of the curing temperature and curing time on the coating property

Curing temperature and time are the other two important factors in determining WVTR results. The effect of the curing temperature on the coating property is shown in Fig. 3(a). The experiments were taken at a fixed APTS content (30 wt%), BPO content (0.4 wt%) and time (30 min) with coat weight fixed at 1 g/m^2. Increasing the curing temperature will give better conversion of the monomers (a decrease in soluble fraction), but only at 80 °C did the WVTR reduced remarkably. This is because the higher temperature will destroy the network structure of the AESO based polymer coating, corresponding to a decrease in contact angle. Similarly, even though the increase in curing time could gradually decrease the soluble fraction in the coated film, increasing the curing time is equal to increasing the hazard degree for the degradation of the formed barrier layer, which causes worse WVTR results, Fig. 3(b). The experiments in Fig. 3(b) were taken at a fixed APTS content (30 wt%), BPO content (0.4 wt%) and reaction temperature (80 °C) with the coat weight fixed at 1 g/m^2.

In summary, based on soluble fraction, contact angle and WVTR results, the suitable AESO/APTS ratio and initiator dosage for the reactive coating were 100:30 and 0.4 wt% respectively, with the

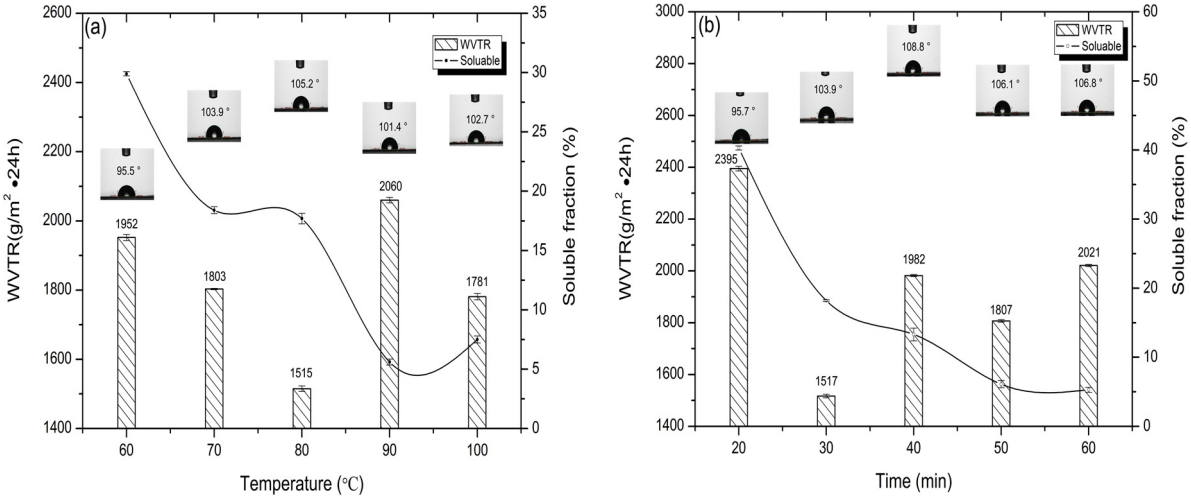

Fig. 3. WVTR, soluble fraction and CA of the coated NFX film with various (a) curing temperatures and (b) curing times.

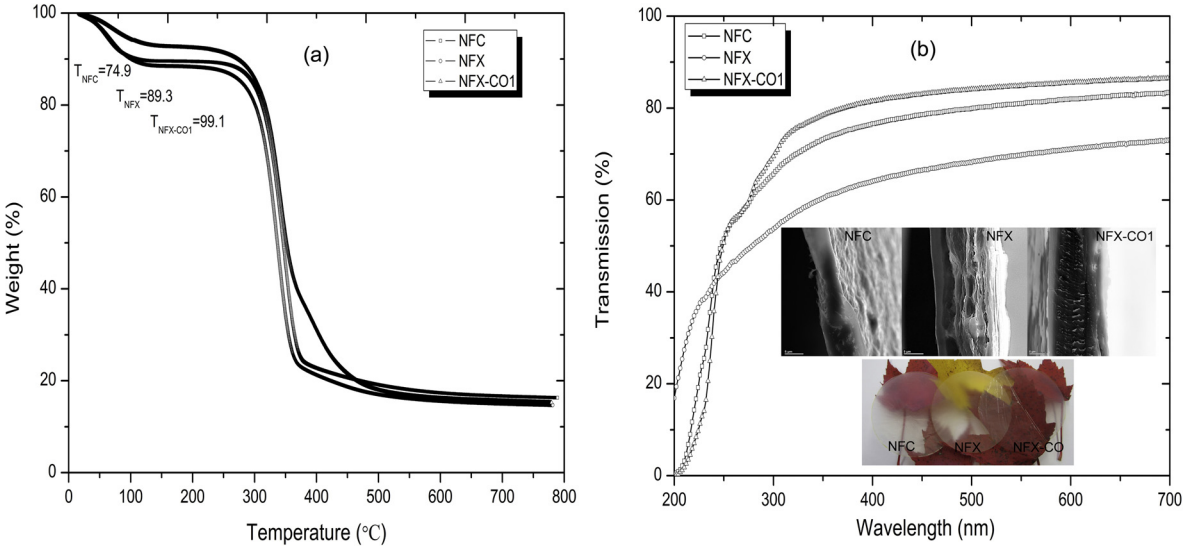

Fig. 4. (a) TGA curve and (b) UV–vis transmittance spectrum of the NFC, NFX and NFX-CO1 film with an SEM image of the cross-section view embedded image in (b).

curing time 30 min and temperature at 80 °C. However, the overall lowering of WVTR was limited regardless of reaction temperature and duration.

3.4. *Effect of the coat weight on the film property*

As mentioned above, a good moisture barrier property of the coating was demonstrated at coat weight 1.0 g/m^2 at the optimum coating formulation. Increasing the coat weight could influence the WVTR directly (Table 2). The reaction conditions include an APTS content of 30% and BPO% of 0.4, with the curing time of 30 minutes and a temperature at 80 °C. Compared to the pure NFC film, adding the beeswax dispersion during film casting could improve the water vapor barrier property only to some extent. On the contrary, after surface reactive coating, the WVTR was reduced significantly, from 1517 (coat weight 1 g/m^2) to 188 (coat weight 5 g/m^2).

On the other hand, the tensile property of the coated NFX films were also higher than that of the NFX and NFC, which might be related to the 3-dimension network structure between the cellulose nanofibrils and AESO-based polymers. The closure of surface pores and the filling of network caused by the AESO reactive coating were also confirmed by the decrease in WVTR when the coat weight increased. However, increasing the coat weight had limited impact on enhancing the tensile strength and the contact angle of the coated films.

Table 2
Summary of the films' properties in terms of WVTR (38 °C, 90% RH), wettability (contact angle) and tensile index.

Sample#	Grammage (g/m^2)	WVTR (g/m^2 24 h)	Contact angle (°)	Tensile index (N m/g)
NFC	10.1 ± 0.5	5088 ± 3	67.3 ± 0.4	44.7 ± 0.6
NFX	10.3 ± 0.7	3918 ± 2	93.7 ± 0.2	50.4 ± 0.7
NFX-CO1	11.7 ± 0.5	1517 ± 5	106.1 ± 0.5	51.6 ± 0.9
NFX-CO3	13.2 ± 0.5	493 ± 7	105.7 ± 0.3	59.2 ± 0.7
NFX-CO5	15.7 ± 0.2	188 ± 8	106.5 ± 0.8	66.3 ± 0.3

3.5. Thermal stability and optical properties of the films

The TGA curve shown in Fig. 4(a) indicates that the degradation of NFC and NFX film began at temperatures lower than that of NFX-CO1. This suggested that the AESO reactive coating can effectively improve the film thermal stability, which is of importance for various applications. Furthermore, all films showed high flexibility and remarkable transparency. As can be seen from Fig. 4 (b), the NFX-CO1 film appeared to be more transparent than the NFX and NFC films. Similar observations have been reported for other NFC composites film (Aulin, Salazar-Alvarez, & Lindstrom, 2012). The high packing density of the NFX-CO1 film revealed by the SEM image resulted in low film porosity, thus decreasing the light scattering or increasing the optical transmittance (Zhu et al., 2010).

4. Conclusions

A moisture-resistant packaging film with low water vapor transmission rate (WVTR) was fabricated based on biodegradable natural resources, such as nanofibrillated cellulose (NFC) and acrylated epoxidized soybean oil (AESO). The reaction between the AESO, APTS and NFC surface were confirmed by FTIR spectroscopy and AFM phase images. After coating and curing at 80 °C for 30 min, a barrier layer was successfully formed on the top of the NFX film, resulting in a significant reduction in WVTR from 5088 to 188 g/m^2 24 h (38 °C, 90% RH). The coating weight at 5 g/m^2 was sufficient to improve the tensile strength of the NFC film. Moreover, the transparency of the NFC film was improved after the AESO reactive coating and meanwhile the contact angle became higher, implying that the surface is more hydrophobic after the coating. The resulting film is promising as a potential biodegradable packaging material.

Acknowledgments

This project was funded by NSERC Innovative Green Wood Fiber Products Strategic Network (Canada), Chinese Scholarship Council (CSC), National Natural Science Foundation of China (NSFC) (Grant No. 31200457) and 973 Project (2010CB732201, China) for funding this project; Authors would also thanks for Prof. M. Sain and Dr. O. Faruk at the University of Toronto for providing NFC.

References

Alves, V. D., Costa, N., & Coelhoso, I. M. (2010). Barrier properties of biodegradable composite films based on kappa-carrageenan/pectin blends and mica flakes. *Carbohydrate Polymers*, *79*, 269–276.

Andersson, C. (2008). New ways to enhance the functionality of paperboard by surface treatment—A review. *Packaging Technology and Science*, *21*(6), 339–373.

ASTM. (2000). *ASTM E96-00. Standard test methods for water vapor transmission of materials*. West Conshohocken, PA, USA: ASTM International.

ASTM. (2003). *ASTM D1653-03. Standard test methods for water vapor transmission of organic coating films*. West Conshohocken, PA, USA: ASTM International.

Aulin, C., Salazar-Alvarez, G., & Lindstrom, T. (2012). High strength, flexible and transparent nan fibrillated cellulose–nanoclay biohybrid films with tunable oxygen and water vapor permeability. *Nanoscale*, *4*, 6622–6628.

Cerpakovska, D., & Kalnins, M. (2012). Barrier and sorption properties of porouspoly(vinylalcohol)–cellulose fibrecomposites. *Proceedings of the Estonian Academy of Sciences*, *61*(3), 178–184.

Coates, J. (2013). Interpretation of infrared spectra, a practical approach. In R. A. Meyers (Ed.), *Encyclopedia of analytical chemistry* (pp. 10815–10837). John Wiley & Sons Ltd.

Çolak, S., & Küsefoğlu, S. H. (2007). Synthesis and interfacial properties of aminosilane derivative of acrylated epoxidized soybean oil. *Journal of Applied Polymer Science*, *104*, 2244–2253.

Grishchuk, S., & Karger-Kocsis, J. (2011). Hybrid thermosets from vinyl ester resin and acrylated epoxidized soybean oil (AESO). *Express Polymer Letters*, *5*(1), 2–11.

Ham-Pichavant, F., Sebe, G., Pardon, P., & Coma, V. (2005). Fat resistance properties of chitosan-based paper packaging for food applications. *Carbohydrate Polymers*, *61*, 259–265.

Kim, J., Seidler, P., Fill, C., & Wan, L. S. (2008). Investigations of the effect of curing conditions on the structure and stability of amino-functionalized organic films on silicon substrates by Fourier transform infrared spectroscopy, ellipsometry, and fluorescence microscopy. *Surface Science*, *602*(21), 3323–3330.

Larsson, K., Berglund, L. A., Ankerfors, M., & Lindström, T. (2012). Polylactide latex/nan fibrillated cellulose bionanocomposites of high nanofibrillated cellulose content and nanopaper network structure prepared by a papermaking route. *Journal of Applied Polymer Science*, *125*, 2460–2466.

Lavoine, N., Desloges, I., Dufresne, A., & Bras, J. (2012). Microfibrillated cellulose-its barrier properties and applications in cellulosic materials: A review. *Carbohydrate Polymers*, *90*, 735–764.

Liu, A., & Berglund, L. A. (2012). Clay nanopaper composites of nacre-like structure based on montmorrilonite and cellulose nanofibers—Improvements due to chitosan addition. *Carbohydrate Polymers*, *87*, 53–60.

López, S. H., & Santiago, E. V. (2013). *Acrylated-epoxidized soybean oil-based polymers and their use in the generation of electrically conductive polymer composites, Chapter. Soybean – Bio-active compounds* (Vol. 11).

Marquez, M., Grady, B. P., & Robb, I. (2005). Different methods for surface modification of hydrophilic particulates with polymers. *Colloids and Surfaces A: Physicochemical and Engineering Aspects*, *266*, 18–31.

Park, H., Xu, S., & Seetharaman, K. (2011). A novel in situ atomic force microscopy imaging technique to probe surface morphological features of starch granules. *Carbohydrate Research*, *346*, 847–853.

Prakash Marana, J., Sivakumar, V., Sridhar, R., & Thirugnanasambandham, K. (2013). Development of model for barrier and optical properties of tapioca starch based edible films. *Carbohydrate Polymers*, *92*, 1335–1347.

Sanchez, J., & Badia, A. (2003). Atomic force microscopy studies of lateral phase separation in mixed monolayers of dipalmitoylphosphatidylcholine and dilauroylphosphatidylcholine. *Thin Solid Films*, *440*, 223–239.

Scott, W. W., & Bhushan, B. (2003). Use of phase imaging in atomic force microscopy for measurement of viscoelastic contrast in polymer nanocomposites and molecularly thicklubricant films. *Ultramicroscopy*, *97*, 151–169.

Sehaqui, H., Liu, A., Zhou, Q., & Berglund, L. A. (2010). Fast preparation procedure for large, flat cellulose and cellulose/inorganic nanopaper structures. *Biomacromolecules*, *11*, 2195–2198.

Spence, K. L., Venditti, R. A., Rojas, O. J., & Hubbe, M. A. (2011). Water vapor barrier properties of coated and filled microfibrillated cellulose composite films. *BioResources*, *6*(4), 4370–4388.

Tammelin, T., Hippi, U., & Salminen, A. (2013). *Method for the preparation of NFC films on supports. WO 2013060934 A2*.

TAPPI. (2006). *Tensile properties of paper and paperboard (using constant rate of elongation apparatus), Revision of T494 om-01*.

Zhang, W., Xiao, H., & Qian, L. (2014). Enhanced water vapour barrier and grease resistance of paper bilayer-coated with chitosan and beeswax. *Carbohydrate Polymers*, *101*, 401–406.

Zhu, H., Parvinian, S., Preston, C., Vaaland, O., Ruan, Z., & Hu, L. (2010). Transparent nanopaper with tailored optical properties. *Nanoscale*, *5*, 3787–3792.